

PERFORMANCE OF SAND DRAINS IN A TEST EMBANKMENT IN SOFT BANGKOK CLAY

A.S. BALASUBRAMANIAM
*Asian Institute of Technology
Thailand*

R.P. BRENNER
*Asian Institute of Technology
Thailand*

G.U. MALLAWAARATCHY
*Asian Institute of Technology
Thailand*

SATAPORN KUVUITJARU
*Asian Institute of Technology
Thailand*

SUMMARY The performance of sand drains at the Naval Dockyard site, Pom Prachul, Thailand was investigated by constructing an instrumented test embankment. The test site is situated at the mouth of the Chao Phraya River in Samutprakarn Province, approximately 20 km south of Bangkok City. The embankment which was built in two stages, was 90 m long, 33 m wide, 2.35 m high and consisted of three sections, namely a section with no drains, a section with drains of 2.5 m spacing, and a section with drains of 1.5 m spacing. The sand drains consisted of small diameter (5 cm) sandwicks and were installed to a depth of 17 m by the displacement method.

A total of 166 piezometers were installed below the test fill area and outside of it. Surface and subsurface settlement points were installed to monitor the settlement along the centre line and the edges of the test embankment. Three hydrostatic profile gages were installed i.e. one along each central cross section of a test section. Also, eleven magnetic movement plates were used with each gage to monitor lateral displacements along the gage. Three inclinometer casings were installed in the centre line of the three test sections.

An extensive program of laboratory oedometer tests and triaxial tests was carried out to determine the necessary soil parameters for the evaluation of immediate and consolidation settlements. The observed pore pressures and settlements are presented here and an attempt is made to compare the observations with the predictions from conventional settlement analysis.

INTRODUCTION

In connection with the construction of a dockyard for the Royal Thai Navy, a test embankment was built in order to evaluate the performance and suitability of sand drains as a means to accelerate consolidation of the soft clay. The test site is located in Samutprakarn Province approximately 20 km south of Bangkok City, at the mouth of the Chao Phraya River.

As in other parts of the Chao Phraya Plain, the sub-soil consists of a thick layer of marine clay followed by numerous alternate layers of sand-gravel and hard clay (see MUKTABHANT, et al, 1967 and MOH et al, 1969). The marine clay is usually divided into three sections, namely an upper layer of weathered clay, about 2 to 4 m thick, followed by a soft clay of up to about 15 m thickness, underlain by stiff clay. Close to the coast, the "soft clay" is particularly soft with a water content close to the liquid limit. At the Pom Prachul site, the surface was initially covered by a dense vegetation cover containing Nipa palms as one of the main elements, and after clearing, the surface layer to a depth of about 2 m contained numerous root holes and pieces of decayed wood. A typical soil profile at the site and the basic properties are presented in Fig. 1.

The test embankment was conceived to consist of three sections, namely one without sand drains and two adjacent sections with drains of different spacing. Sand drains were of the displacement type with wicks of 5 cm diameter. Figures 2 and 3 illustrate the plan and elevation of the test embankment with instrumentation. The spacings chosen for the sand drains were 1.5 m and 2.5 m. The sand drains extend to the full depth of soft clay, i.e. 17 m.

SAMPLING AND INSTALLATION OF FIELD INSTRUMENTS

A total of eight boreholes were drilled for the purpose of soil identification, index properties and laboratory tests. Sampling was carried out by means of piston samplers. In order to create a reference point for settlement observations, a bench mark was constructed at about 120 m from the test area. It consisted of a 2½ inch galvanised pipe penetrating into

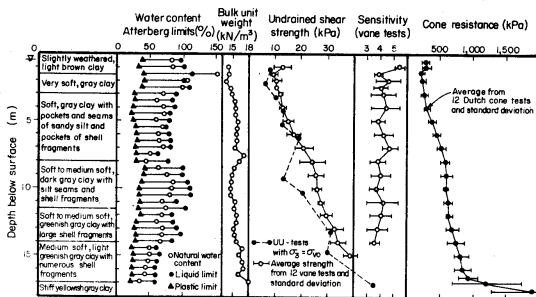
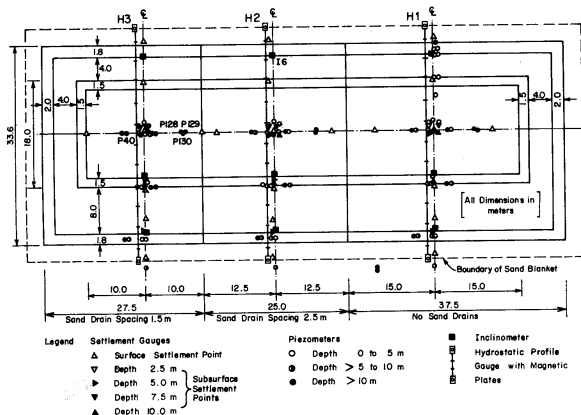


Fig. 1 General Properties of Pom Prachul Clay



Piezometers

A total of 166 piezometers were installed below the test fill area and outside of it. "Dummy" piezometers were installed in the region beyond the influence zone of the embankment load, and thus had the function to serve as reference gages, while active piezometers were used to indicate the pore pressure in the regions with an excess with respect to the steady-state conditions.

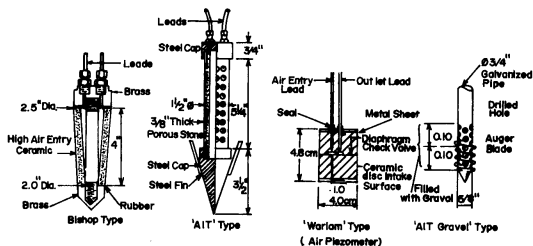
The AIT-type piezometer was the most frequently employed (see Figs. 4a & 4b). It consists essentially of a cylindrical porous stone in a perforated steel pipe attached to a steel cone at the lower end and a steel cap at the upper end. The "Bishop" type has a ceramic element of a high air entry value and was used after it was found that the piezometer lines required frequent de-airing, probably due to a rather high gas content in the soil. The gravel type piezometer is designed for cohesionless soils with high permeability and was installed in some of the sand wicks. The closed hydraulic system has the advantage of a small response time as it can be monitored through a null indicator and a screw control. This type was employed for most of the active gages particularly those under the embankment. Piezometer tips for such a system have twin-walled outlet tubes to facilitate de-airing. Finally, the air piezometer system was used as a check in order to have an independent comparison of the pore pressures read from the AIT type and the Bishop type gages.

All piezometer tips, except the gravel type, were installed in the soft clay stratum. Piezometers with an AIT type tip were installed by simply pushing them manually into the ground to the required depth by means of a special adaptor and a steel pipe. For the Bishop and the Warlam-type a borehole had to be drilled and the piezometer tips were embedded in sand and then sealed by a bentonite plug. Finally, the gravel type piezometer tip was installed by augering it down within the sand drain, making use of the specially provided auger blades. After installation each closed system piezometer was carefully de-aired using a portable de-airing unit and a pressure of 20 psi to flush the lines. Later on, this procedure was repeated each time before taking readings on the mercury manometer of the monitoring board. The resting period between de-airing and reading was not less than 24 hours. In the case of open stand-pipe piezometers, a water level indicator was used to record the position of the water table in the tubes.

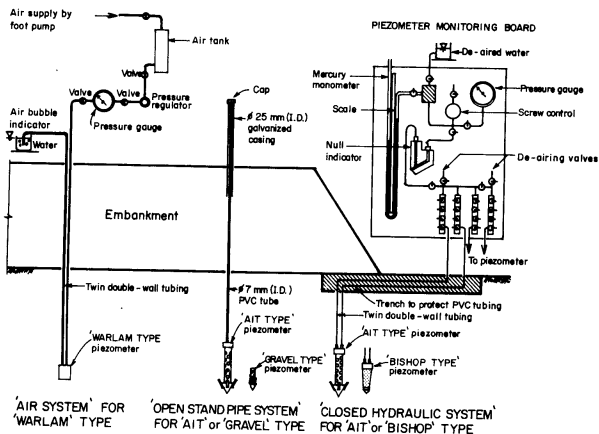
In order to record fluctuations in ground water table in the area around the embankment, six observation wells were built. Readings from the observation wells when compared to those from the dummy piezometers could indicate deviations from a hydrostatic pressure distribution, an important factor when interpreting the active piezometer records.

Settlement Gages

Settlement points installed were of two types, namely surface settlement points and subsurface settlement points. Surface settlement points consisted of a 16 mm ϕ steel rod connected to a 0.40 x 0.40 m base plate and



(a)



(b)

Fig. 4 Piezometers used at Pom Prachul Site

protected by a 19 mm diameter casing. The sub-surface type consisted of a 25 cm diameter steel screw head connected to a 16 mm diameter steel rod. These were screwed into the ground by means of a 19 mm internal diameter steel tube which was attached to the screw head by a keyway. After installation to the desired depth, the outer tube was lifted from the keyway by about 20 cm. The tube was left in the ground and filled with oil to eliminate the dragdown force on the inner rod caused by the clay compression. The details of these settlement points are illustrated in Fig. 5. Measurements of settlements were made on the top of the rods using a staff and an optical level. The readings were referred to the benchmark, the elevation of which was taken as +2.231 m.

Hydrostatic Profile Gage

The hydrostatic profile gage comprises a probe containing a flexible bladder which is connected by a tube to an electric pressure transducer in the tube drum. The tube and bladder are filled with water. A second tube equalizes pressures in the probe and in the drum. Changes in level at the probe result in changes in negative pressure at the transducer. The probe is pulled or pushed along an access tube and responds to undulations in the tube giving a complete record of the profile. A second probe (read switch probe), separated from the bladder probe by 1 m of cable, is operated on a read switch and magnet principle and is able to detect the lateral movement of permanent ring magnets positioned along the access tube.

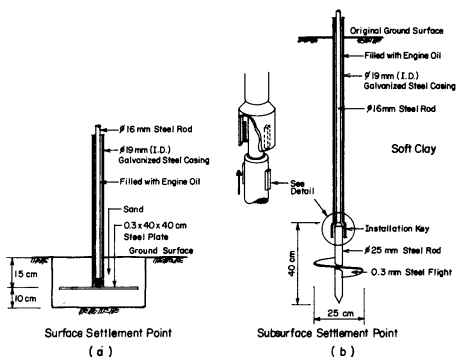


Fig. 5 Surface and Sub-surface Settlement Points

The installation procedure for this device is illustrated in Fig. 6. In each of the three sections a trench, about 0.4 to 0.6 m deep, was dug and leveled out with sand. The access tube was then placed into this trench after having been fitted with the required number of ring magnets. After carefully positioning, aligning and leveling the magnetic plates and the access tube, the trench was backfilled with layers of compacted sand. At both ends of each access tube, concrete pads on short wooden piles were cast, embedding the ends of the access tube which were surrounded by steel pipe sleeves. A string which was later used to pull the probe through the tube was then inserted.

Figure 2 shows the location of the three access tubes and the position of the eleven magnetic movement plates. The lateral displacement of these plates will correspond to the lateral displacement of the adjoining soil. The vertical displacement at these points or at any other regular interval can then be monitored by pulling the twin probe through the access tube.

Inclinometers

Three inclinometer casings were installed in the centre line of each of the three test sections. These casings consisted of 58 mm outside diameter plastic tube sections of 3 m length with four keyways to align the probe in the required direction of measurement. The probe contained a strain-gaged pendulum in its interior which could sense changes in the tube curvature. A readout unit with a meter display giving the position angle of the torpedo was used. The calibration of the torpedo was checked frequently on a specially built calibration frame.

The installation procedure is pictured in Fig. 7. First a tube to a depth of about 25 m was drilled. The portion in the soft clay was supported by a casing. Then the section of the borehole in the stiff clay was filled with a bentonite cement mixture of 1:1. The inclinometer access tube was then assembled piece by piece by means of couplings and rivets, and simultaneously lowered into the borehole. To overcome buoyancy, the assembled tube section was filled with water. When the tube had reached the bottom of the borehole, the borehole casing was withdrawn and the gap between the access tube and borehole wall was filled with a 3:1 bentonite cement slurry. It was found by previous investigations that this mixing ratio developed a strength similar to the one of the soft clay, and therefore, would not provide additional stiffness to the tube. Support to the casing was also provided by collapsing sections of the borehole.

Initial measurements were carried out before any fill was placed. Readings were taken at 0.5 m intervals. The torpedo was first lowered down to the bottom of the hole and readings were then taken while pulling it up. For each access tube two profiles, i.e. in the N-S and in the E-W direction, were recorded.

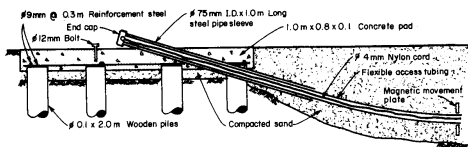


Fig. 6 Installation of Hydrostatic Profile Gage

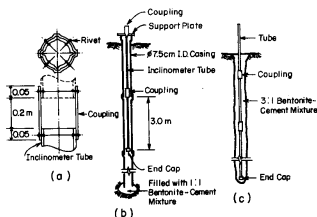


Fig. 7 Installation of Inclinator Casing

RESULTS FROM FIELD INSTRUMENTATION

Piezometer Observations

A typical record of the piezometer readings is shown in Fig. 8. The three piezometers were installed in different test sections but at corresponding positions and enable, therefore, a direct comparison of performance. The pressures shown for the active piezometers are total values, i.e. the excess pore pressure plus the hydrostatic pressure at the piezometer tip level based on the ground water level in the reference observation well. Also, given in the figure are the time variations of the water level in the observation well used as reference and the record of the dummy piezometer installed at the same depth as the active piezometer. If there were no deficiency in static pore pressure due to deep well pumping then these two lines should more or less coincide. On top of Fig. 8 the vertical stress due to embankment loadings is given for the location of each piezometer tip. These

stress increments were calculated by using Boussinesq's equations for an elastic half space.

All piezometer readings are fairly consistent. Although de-airing had been carried out at regular intervals, it is suspected that at times gas had accumulated much more rapidly than expected. A look at the records of the piezometers installed at greater depths i.e. 10 m to 15 m indicated that large excess pore pressures resulted if the dummy piezometers were taken as the reference. These dummy piezometers showed a distinct draw-down effect (see Fig. 9). If the absolute pore pressures of the deep piezometers under the embankment are compared with the hydrostatic pressure due to the ground water level as revealed by the observation wells (with no allowance for draw-down effects), then the excess pore pressures are largely reduced and are comparable with the induced stresses. In other words, this would indicate that below the embankment the draw-down effect is non-existing probably due to the recharging action of the sand drains.

In order to clarify this situation a large number of additional piezometers was installed and the results obtained is shown in Fig. 10. In this figure the variation in draw-down in the east direction is shown and it can be seen that the recharging effect extends about 15 m from the edge of the sand drain area.

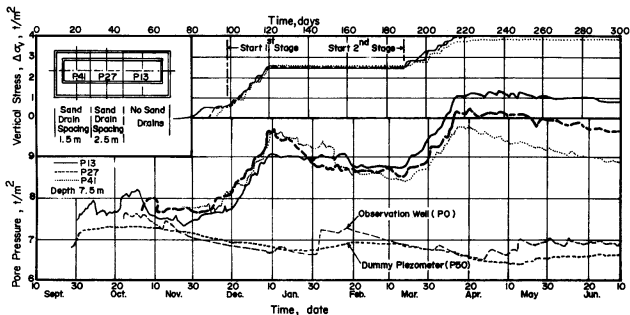


Fig. 8 Typical Piezometer Readings

Settlement Observations

Settlement records for 47 active settlement points have been studied and typical cases are plotted in Fig. 11. On the top of the graph, the time

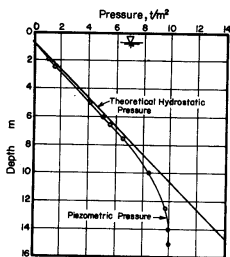


Fig. 9 Piezometric Draw-Down due to Deep Well Pumping

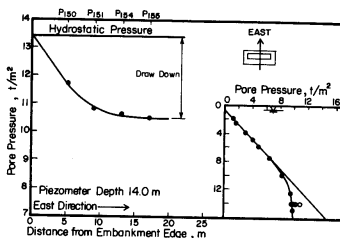


Fig. 10 Groundwater Recharge by Sand Drains

variation of vertical stress at the location of the settlement point due to embankment loading is shown.

From the settlement measurements it appeared that the major parts of the settlement took place in the uppermost 5 m of the soil profile. Also there was no difference in the settlement behaviour of the no drain section and the section with 2.5 m drain spacing. The section with the 1.5 m spacing, however, exhibited significantly larger settlements.

Results from Hydrostatic Profile Gages

Figure 12 shows the results obtained from a hydrostatic profile gage in the centre of one section. The shapes of the settlement profiles are very similar and are in agreement to those obtained from the surface settlement points. Figure 13 illustrates the development of lateral movements as recorded from the position of the magnetic plates along the access tube.

Inclinometer Observations

Typical lateral displacements as observed in the E-W direction are shown in Fig. 14. All lateral movement profiles of the six inclinometers along the edges of the fill exhibit a maximum in the region of 1.5 to 2.5 m depth, while the maximum of the three inclinometers in the center portion of the fill occur at about 4 m depth. The values of these maximum displacements are of the same order of magnitude as those recorded from the movement of the magnetic plates although these plates were only at about 0.5 m depth. Again, a particular effect of the sand drains on lateral displacement cannot be noticed from the slope indicator observations. The zone of maximum displacement also coincides with the softest zone of the soil profile.

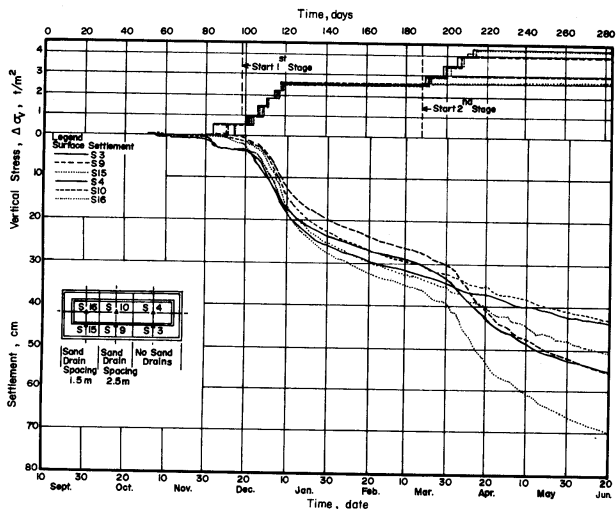


Fig. 11 Typical Settlement Point Readings

In-situ Permeability Measurements

In-situ permeability was measured during the preliminary investigation stage by the auger hole method. These tests were carried out in 4-inch diameter boreholes in the soft clay and 3-inch diameter boreholes in the stiff clay and sand.

For the permeability tests the borehole was cased with 3-inch diameter casing. The mud slurry was washed from the borehole until the water in the borehole was clean. Then water was filled in the 3-inch casing up to its top which was about 2 m above ground surface. In the constant head test the water level in the casing was maintained constant by a continuous flow of water from a container of known volume. The rate of flow required to maintain the water level at a constant value was measured. In the falling head test, the water head drop in the 3-inch casing was measured with time. The permeabilities determined by these tests are presented in Fig. 15.

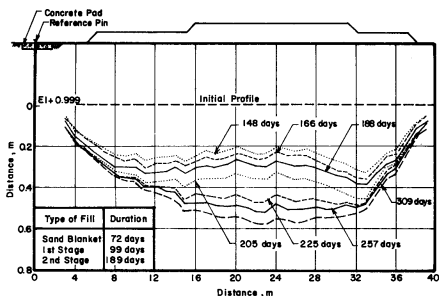


Fig. 12 A Typical Hydrostatic Profile Gage Record

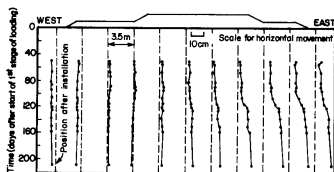


Fig. 13 Records of Lateral Movement by Magnetic Plates

CONSOLIDATION TESTS

Testing Program

The results of six series of oedometer tests were used in this study. The three types of consolidometers used were of Lever Arm, Anteus and Bishop type.

Consolidation test series SC. - This series consisted of 7 tests conducted on samples taken from a depth of 1 to 16 m. The in-situ overburden pressure of the samples varied from 0.9 to 14 t/m². All tests were carried out in the Lever Arm type consolidometer. A load increment ratio of 1.0 and a load increment duration of 24 hours were used for these tests.

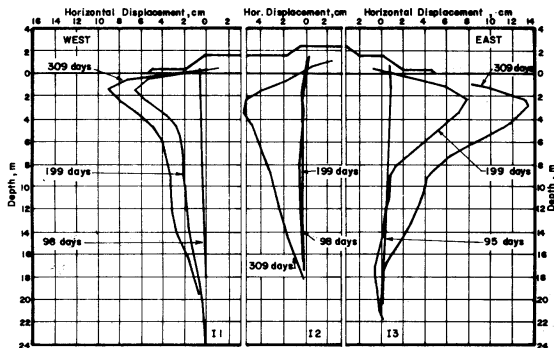


Fig. 14 Typical Lateral Displacements from Inclinomometer Measurements

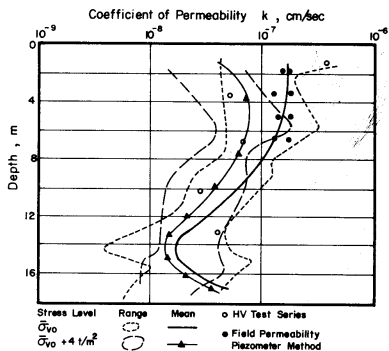


Fig. 15 Permeability of Pom Prachul Clay

Consolidation test series AC. - Seven consolidation tests were carried out in the Anteus consolidometer with pore pressure measurements. The sample depths varied from 1.75 to 17.3 m. For all tests the first increment of load corresponded to $1/4$ th of the overburden pressure. Subsequently, the consolidation pressure was increased to the in-situ overburden pressure in steps as follows: $\bar{\sigma}_{vo}/4$, $\bar{\sigma}_{vo}/2$, $3\bar{\sigma}_{vo}/4$ and $\bar{\sigma}_{vo}$. The next two consolidation pressures corresponded to an increase in stress of 1 and 2 t/m^2 above the in-situ overburden pressure. The final four increments were such that the consolidation pressures corresponded to $2\bar{\sigma}_{vo}$, $4\bar{\sigma}_{vo}$, $8\bar{\sigma}_{vo}$, and $16\bar{\sigma}_{vo}$.

Consolidation test series BC. - Consolidation test series BC was identical to series AC, except that tests were performed in the Bishop consolidometer with pore pressure measurements.

Consolidation test series SI. - The test series SI was performed in the Lever Arm consolidometer, but small increments were used, so that the maximum past pressure could be determined accurately. The load increment duration was 30 minutes only. Altogether nine tests were carried out on samples taken from a depth of 1.6 m to 15.6 m.

Consolidation test series LC. - These tests were performed in the Lever Arm consolidometer. Only three tests were carried out on samples from depths of 5.4, 10.6 and 15.7 m. These samples were consolidated initially to the in-situ overburden pressure and then a single increment of 4 t/m^2 was applied. The in-situ overburden pressure was applied for one day and the subsequent 4 t/m^2 was applied for about 35 to 41 days.

Consolidation test series HV. - These tests were also carried out in the Lever Arm consolidometer. Ten tests were done five of which were performed on samples which were trimmed in the usual manner. The other five tests were conducted on samples which were trimmed in such a manner that the loading in the laboratory could be carried out in a direction perpendicular to the vertical orientation of the samples in the field. Thus the latter series can be used to evaluate the coefficient of consolidation of the samples corresponding to the horizontal flow in the field.

Stress - Strain Relationships

The axial strain vs. pressure (log scale) plots obtained from consolidation test series AC are given in Fig. 16. The virgin compression curves for all samples are found to be nearly parallel.

Maximum Past Pressure

The variation with depth of the maximum past pressure determined from the consolidation tests are shown in Fig. 17. The values lie within a narrow band showing an increase in maximum past pressure with depth. The range of maximum past pressure values was plotted along with the different loading conditions, i.e. in-situ overburden pressure under the first stage loading and under the second stage loading. The maximum past pressure range is more or less parallel to these loading lines. For a depth of about 6 m, the loading is in excess of the maximum past pressure and higher settlements can be expected. Then to a

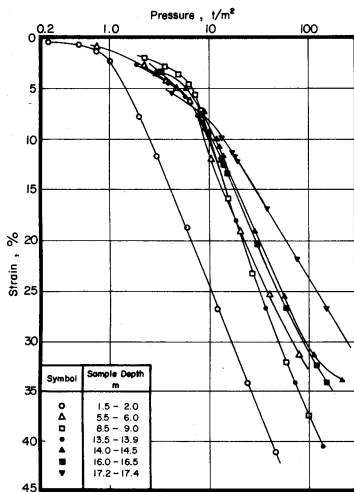


Fig. 16 Compression Characteristics of Pom Prachul Clay

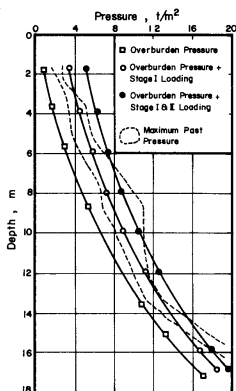


Fig. 17 Maximum Past Pressure for Pom Prachul Clay

depth of about 12 m, the loading stages just straddle the $\bar{\sigma}_{vm}$ range. From 12 m to 15 m the maximum past pressure is exceeded by the loading.

The variation in the range of compression indices with depth is shown in Fig. 18. The variation was plotted for values of C_c at the in-situ overburden pressure and for those under the embankment loading. The corresponding compression ratios are shown in Fig. 19. From these diagrams it can be seen that under the in-situ overburden pressure C_c is almost of constant value (~ 0.3) for a depth less than 10 m and has a higher value (~ 0.45) below that depth. Below 16 m a decreasing trend of C_c is indicated.

Coefficient of Consolidation

The coefficients of consolidation were determined from the results of the consolidation test series SC, AC & BC. Casagrande's log time fitting method and Taylor's square root time fitting method were used. For test series AC and BC in which pore pressures were measured, the coefficient of consoli-

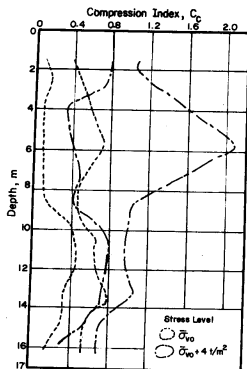


Fig. 18 Compression Index for Pom Prachul Clay

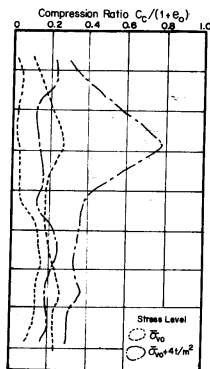


Fig. 19 Compression Ratio for Pom Prachul Clay

dation was also determined by means of the pore pressure dissipation curve. The variation of the coefficient of consolidation with depth is shown in Fig. 20. The values have been plotted for stress levels corresponding to the in-situ overburden pressure and the embankment loading.

SETTLEMENT ANALYSIS OF TEST EMBANKMENT

Stress Distribution

In this study the stress distribution under the embankment was calculated by two methods, namely Gray's method and Poulos' method. The average unit weights were 1.62 t/m^3 for the sand blanket, 1.86 t/m^3 for the first stage loading and 1.92 t/m^3 for the second stage loading. The results are presented in Fig. 21.

Immediate Settlement

The stress - strain curves of the undrained creep tests were used to compute the immediate settlement under the embankment. For this, the undrained strain was multiplied by the thickness of the layers into which the clay stratum was divided to suit the sample depths. In the undrained creep test the value of the strain is a function of time. Therefore, to arrive at a reasonable value corresponding to the field loading condition the following approach

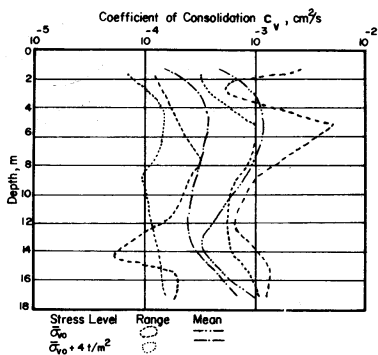


Fig. 20 Coefficient of Consolidation for Pom Prachul Clay

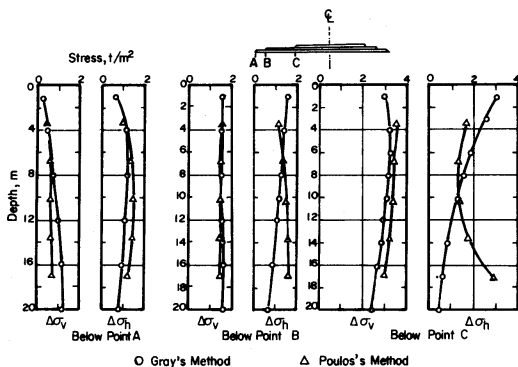


Fig. 21 Stress Distribution Below Embankment

was used: The time taken to apply the load was assumed to be proportional to the square of the thickness of a layer. On this basis a period of one day in the field corresponded to 4 minutes for the laboratory sample. Thus from the undrained creep test results, the strains at 4 minutes were taken to compute the immediate settlement. Figure 22 shows the computed immediate settlements along the centre line of the embankment. From the figure, it can be seen that very little immediate settlement occurs below about 11 m. The immediate surface settlement under the first stage loading and the second stage loading was computed to be 3.6 cm and 11.5 cm respectively.

Consolidation Settlement

The total primary consolidation settlement under the embankment loading was calculated using the stress - strain curves from the consolidation test series. Figure 23 shows the variation of primary settlement with depth as computed above. The settlements computed from test series BC are found to be high and deviated widely from the other results. Figure 24 shows the ratio of observed to calculated settlements. The observed settlements are found to be higher than the computed settlements.

From the observed settlement reading the compression of each 2.5 m layer within the no sand drain area and the two sand drain areas were calculated and plotted against time. This is shown in Fig. 25, and it can be seen that for the top 5.0 m layer the rate of settlement is faster in the 1.5 m spaced sand drain area. However, below 5.0 m depth, no significant improvement is noted with the use of sand drains.

Rate of Settlement

The time rate of settlement was calculated according to one-dimensional consolidation theory. The settlement of 2.5 m thick layers corresponding to the location of settlement measuring points was considered. The maximum drainage path was taken as the effective radius of the sand drain installation pattern. At Pom Prachul, the sand drain installation follows a rectangular pattern and the effective diameters for the 1.5 m spaced and 2.5 m spaced areas are 1.7 m and 2.83 m respectively. The solutions derived by SCHIFFMAN (1958) were used in calculating degrees of consolidation. As a first approximation, it was assumed that these solutions were applicable although the directions of settlement and drainage were not the same.

Figure 26 shows the plot of settlement vs time for the 2.5 m layers of soil in the 1.5 m spaced sand drain area. In the diagram are also plotted the settlements calculated as explained above for different assumed values of c_v . The immediate settlement as calculated before has been added. From the figures, it can be seen that for the top 2.5 m layer of soil the observed settlements were very much greater than those calculated during the first stage of loading. The greater rate of settlement in the field may be due to the presence of root holes, fissures, etc., near the surface which forms shorter drainage paths to accelerate the consolidation process. However, after the second stage of loading the settlement curve, obtained using a c_v value of $20 \times 10^{-4} \text{ cm}^2/\text{sec}$, was close to the observed curve.

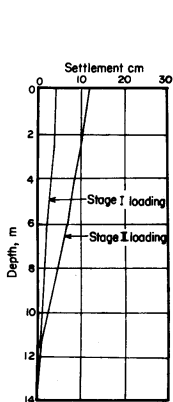


Fig. 22 Immediate Settlement below Embankment

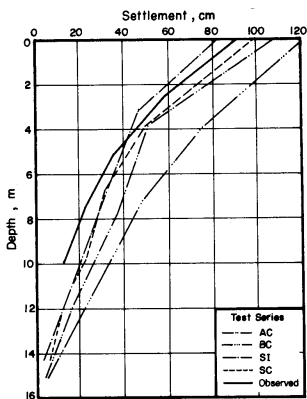


Fig. 23 Consolidation Settlement below Embankment as Calculated from Terzaghi Theory

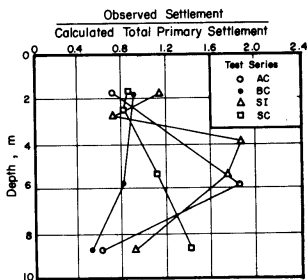


Fig. 24 Ratio of Observed to Calculated Settlement (Terzaghi Theory)

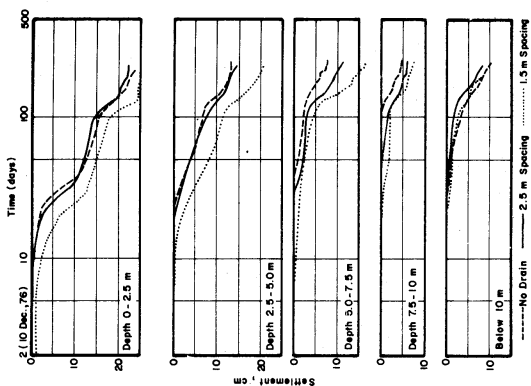


Fig. 25 Comparison of Settlement-Time Records in Sections with and without Drains

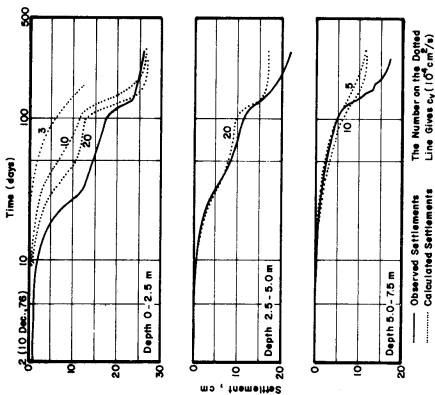


Fig. 26 Observed and Calculated Settlements (1.5 m Spaced Sand Drain Section)

Figure 27 shows the results for the 2.5 m spaced sand drain area. For the layer between 2.5 to 5.0 m the computed settlement curve, with a c_v value of 20×10^{-4} cm²/sec agreed fairly well with the observed curve. For the layer between 5.0 to 7.5 m, a c_v value of about 5×10^{-4} cm²/sec gave good agreement with the measured settlements during the first stage loading. However, after the second stage loading the measured values were very much greater than those predicted.

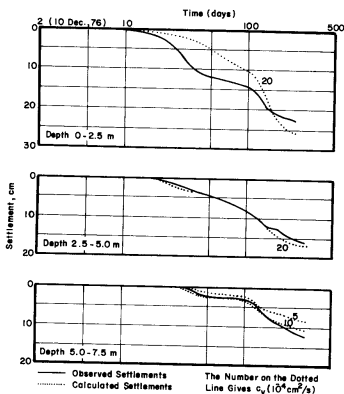


Fig. 27 Observed and Calculated Settlements (2.5 m Spaced Sand Drain Section)

CONCLUSIONS

A detailed description of the instruments used in a test embankment with sand drains is given and the typical observations recorded are described. Laboratory tests were carried out to evaluate the necessary soil parameters for the estimation of the settlements. The following conclusions are reached:

1. There is a large scatter in the values of the soil parameters determined by means of laboratory tests, probably due to the frequent presence of shell fragments, silt and sand seams in the soft clay.
2. Field permeability values were of the same order of magnitude as the vertical permeability determined in the laboratory. The horizontal permeability was higher than the vertical permeability.

3. Within the top 2.5 m, the observed rate of settlement was very much faster than the predicted one, probably due to the presence of root holes, fissures, etc. near the surface of the soft clay.
4. The settlements below 7.5 m in all three test zones are almost the same indicating that the sand drains are not very effective at deeper depths.
5. The coefficients of consolidation determined to fit the observed settlements were about twice the values determined from laboratory tests.
6. There is a piezometric draw-down below a depth of 6 m due to deep well pumping in the region. This is recharged by the installation of the sand drains.
7. The observed settlements were greater than those obtained by the one-dimensional calculation.

ACKNOWLEDGEMENTS

The authors wish to thank Dr. Edward W. Brand, Prof. John Hugh Jones, Mr. Ruangvit Chotivittayathanin, Mrs. Vatinee Chern for their assistance in carrying out the work presented here.

REFERENCES

- MOH, Z.M., NELSON, J.D. and BRAND, E.W. (1969), "Strength and Deformation Behaviour of Bangkok Clay", Proc. 7th Int. Conf. on Soil Mechanics and Foundation Engineering, Mexico, Vol. 1, pp. 287-295.
- MUKTABHANT, C., TEERAWONG, P. and TENGAMNUAY, V. (1967), "Engineering Properties of Bangkok Subsoils", Proc. Southeast Asian Conference on Soil Engineering, Bangkok, pp. 1-7.
- SCHIFFMAN, R.L. (1958), "Consolidation of Soil under Time Dependent Loading and Varying Permeability, Proc. HRB No. 27, 1958, pp. 584-617.